Department of the Navy
Office of Naval Research
Contract N6onr-244, Task Order II

NOTE ON THE EFFECT OF MERIDIAN CURVATURE

Supplement to
POTENTIAL FLOW THROUGH RADIAL FLOW TURBOMACHINE ROTORS

A. J. Acosta

Hydrodynamics Laboratory
California Institute of Technology
Pasadena, California

Project Supervisor:
A. J. Acosta

Approved by:
A. Hollander

Report No. E-19.5
April, 1954

Abstract

The effect of meridian curvature in a centrifugal impeller is estimated by assuming that the meridian streamlines may be replaced by "two-dimensional" surfaces of revolution. For the analysis, a shape was chosen that made the potential flow on this surface easy to solve. It is found that the slope of the streamline at the blade inlet is quite important for the determination of the flow-rate for shockless entry. If the solidity is somewhat greater than unity, the shockless condition is relatively independent of the exit inclination. The head, however, shows little dependence on the inlet, but is a function of the exit slope.

Introduction

The theoretical operating characteristics of radial flow centrifugal pump impellers with small variations in breadth and vane angle have been worked out previously.[1] These calculations were intended primarily for straight radial meridian profiles although it was shown how they could be applied (in the case of small constant breadth) to conical shapes. It is well known that most impellers of the so-called Francis type have appreciable meridian curvatures in which the exit is more or less radial and the inlet may be nearly axial. This present note is a continuation of the work in Reference 1 and is intended to show the effect of this curvature on the characteristics of the impeller. For this purpose, the meridian flow is assumed to occur on a "two-dimensional" surface of revolution. Furthermore, two adjacent meridian streamlines are presumed to be a constant infinitesimal distance dh apart (Fig. 1), so that complex variable theory can be used.

If dh is not constant, the stream function will not satisfy Laplace's equation and the problem becomes much more difficult. However, in this event, further corrections can still be made as are indicated in (1). The impeller may be thought of as consisting of a number of such surfaces, so that a "psuedo-three-dimensional" solution could be constructed for any given design. In the development that follows, however, only one meridian stream surface will be considered.

Formulation of the Problem

Consider the two-dimensional surface of revolution shown in Fig. 2 where the equation of the surface is

$$z = f(R) . \tag{1}$$

The flow on this surface is assumed to satisfy all of the requirements of a potential flow, i.e., it is frictionless, irrotational, and incompressible. Thus, if F is the potential of the flow, then it must satisfy Laplace's equation on the surface. In curvalinear coordinates x_1, x_2, this equation is[2]

$$\frac{\partial}{x_1}\left(\frac{h_2}{h_1}\frac{\partial F}{\partial x_1}\right) + \frac{\partial}{\partial x_2}\left(\frac{h_1}{h_2}\frac{\partial F}{\partial x_2}\right) = 0 . \tag{2}$$

Let $x_2 = \theta$ be the polar angle, and $x_1 = s$, the arc distance along a meridian (θ = constant). Since an element of distance is

$$dS^2 = ds^2 + R^2 d\theta^2$$

then

$$h_1 = 1 ; \qquad h_2 = R .$$

Thus

$$R\frac{\partial}{\partial s}\left(R\frac{\partial F}{\partial s}\right) + \frac{\partial^2 F}{\partial \theta^2} = 0$$

where $R = \bar{R}(s)$ is the question to be solved. It is more convenient to map the (s, θ) coordinates into polar coordinates (y, θ), where Eq. (2) assumes the form

$$y\frac{\partial}{\partial y}\left(y\frac{\partial F}{\partial y}\right) + \frac{\partial^2 F}{\partial \theta^2} = 0 . \tag{3}$$

The connection between s, R, and y is

$$\frac{dy}{y} = \frac{ds}{R} = \frac{dR}{R} \left[1 + \left(\frac{dz}{dR}\right)^2\right]^{1/2}$$

or

$$\ln y = \int \frac{dR}{R} \left[1 + \left(\frac{dz}{dR}\right)^2\right]^{1/2} . \tag{4}$$

Also

$$s = \int dR \left[1 + \left(\frac{dz}{dR}\right)^2\right]^{1/2} . \tag{5}$$

The relation between the (s, θ) and (y, θ) planes is a conformal one so that an impeller blade of constant angle γ defined by

$$\tan \gamma = R\, d\theta/ds$$

is mapped into a logarithmic spiral in the (y, θ) plane.

Boundary Conditions

In the (s, θ) plane let V_{ns} be the normal velocity component and V_{ny} be the normal component in the (y, θ) plane. Then

$$V_{ny} = V_{ns} \frac{\partial s}{\partial y} = V_{ns} \frac{\partial s}{\partial R} \frac{\partial R}{\partial y} , \tag{6a}$$

or

$$V_{ny} = V_{ns} \frac{R}{y} . \tag{6b}$$

For an impeller the total flow is composed of the through flow and the displacement flow. The through flow consists of the flow originating from a source vortex in the (y, θ) plane and is mapped onto the physical plane by Eqs. (4), (5). The displacement flow arises from rotation of the vanes with no net discharge. At any point on the blade surface the normal velocity component must satisfy the condition (Fig. 2)

$$V_{ns} = R\omega\cos\gamma \ .$$

Thus,

$$V_{ny} = \frac{R^2}{y}\omega\cos\gamma \tag{7}$$

is the boundary condition imposed in the (y, θ) plane. In this plane, the blade will appear as a logarithmic spiral for which suitable transformations are available.

Applications

A. Francis-type Impeller

In this type of impeller the exit is nearly radial and the inlet may vary anywhere from axial to near radial as seen in Fig. 1. From Eqs. (4) and (7) it is seen that rather difficult boundary conditions may occur in the (y, θ) plane depending on the exact shape of the streamline contour. In this work the item of major interest is the axial inclination of the inlet (δ_1) and not the particular shape by which this slope is achieved. It is supposed for the present that the details of the profile shape are not of crucial importance, particularly for impellers of high solidity. Later, this contention will be supported by comparing the results of two different shapes.

In view of these remarks it seems reasonable to choose that contour which will give the simplest boundary condition in the (y, θ) plane and still give a streamline shape that has a continuous smooth curvature from inlet to exit. A simple relation that still preserves the axial to radial transition is

$$y^2 = R^2 - R_i^2 \tag{8}$$

where R_i is a constant. Equation (7) gives

$$V_{ny} = \omega \cos\gamma \left[\frac{R_i^2}{y} + y \right] . \tag{9}$$

The first term is the boundary condition for an axial impeller (or cascade) of straight blades. The second term is the boundary condition for a strictly radial impeller.

The relation between z and R is given by Eq. (4), i.e.,

$$\frac{dy}{y} = \frac{dR}{R} \left[1 + f'^2 \right]^{1/2}$$

or with Eq. (8)

$$f'(R) = \frac{dz}{dR} = \left[\frac{R^4}{(R^2 - R_i^2)^2} - 1 \right]^{1/2} . \tag{10}$$

The integral of Eq. (10) is plotted in Fig. 3 and the angle δ_1 is given in Fig. 4 as a function of R/R_i. The constant, R_i, is the value of the radius for which the streamline becomes axial. Although the shape given in Fig. 3 has a much smaller radius ratio than is typical of pump designs, it will be seen that it is still useful for the determination of the effect of δ_1.

1. Displacement Flow

In order to present the results in dimensionless form, consider the new variable

$$r = \frac{y}{R_2} \Bigg/ \left[1 - \left(\frac{R_i}{R_2} \right)^2 \right]^{1/2} . \tag{11}$$

Then

$$V_{nr} = \frac{V_{ny}}{R_2} \cdot \frac{d(y/R_2)}{dr} \tag{12}$$

or

$$V_{mr} = \cos\gamma \left\{ \frac{(R_i/R_2)^2}{r} + \left[1 - \left(\frac{R_i}{R_2} \right)^2 \right] r \right\} . \qquad (13)$$

With these substitutions $r = 1$ when $R/R_2 = 1$, and all velocities are now expressed in terms of the tip speed R_2 of the impeller.

The blades appear as logarithmic spirals in the (r, θ) plane, and because of that fact this plane can be easily transformed into one in which the blade system appears as a circle. In this latter plane the solution to the boundary value problems given by Eq. (13) is relatively simple. As previously noted, the second term represents the conventional radial flow theory whereas the first term is the same as that due to a source flow at the origin. Both of these results are given in Ref. 1 in a form most useful for presentation here.

In this way the effect of meridian curvature can be obtained by "fairing together" two known solutions in the (r, θ) plane by means of Eq. (13). The relation between the actual geometry and the transformed radial plane (r, θ) is given by Eqs. (4), (5), and (11).

The solution of the second term is given by Eq. (11) in Ref. 2. If subscript (2) denotes the exit and (1) the inlet, then the tangential velocity in the circle plane due to this term is

$$\left.\begin{aligned} V_{d_2} &= - \frac{\left[1 - \left(\frac{R_i}{R_2} \right)^2 \right]}{N \rho_2} \left[\frac{w_c}{w_o - 1} \right]^{\bar{q}} \left[\frac{\bar{w}_o}{\bar{w}_o - 1} \right]^{q} \left[2F_1 + \frac{N}{\cos\gamma} (\rho_2 - 2\cos\gamma) F_2 \right] \cos\gamma \\ V_{d_1} &= \frac{\left[1 - \left(\frac{R_i}{R_2} \right)^2 \right]}{N \rho_1} \left[\frac{w_c}{w_o - 1} \right]^{\bar{q}} \left[\frac{\bar{w}_o}{\bar{w}_o - 1} \right]^{q} \left[2F_1 - \frac{N}{\cos\gamma} (\rho_1 - 2\cos\gamma) F_2 \right] \cos\gamma \end{aligned}\right\} \qquad (14)$$

where w_o, ρ are constants that occur in the transformation of the (r, θ) into the circle plane. The constant q is a function of the number of blades N

and the blade angle γ and F_1, F_2 are hypergeometric functions given by Eqs. (19) in Ref. 1.

The tangential velocity of the first (or source flow) term is readily obtained in the circle plane by letting $m = -2$ or $N' = \infty$ in Eq. (35), Ref. 1, to obtain

$$V'_{d_2} = - \frac{2\cos\gamma}{N \rho_2} \left[\frac{R_i}{R_2} \right]^2$$

$$V'_{d_2} = \frac{2\cos\gamma}{N \rho_1} \left[\frac{R_i}{R_2} \right]^2 \qquad (15)$$

The dashes refer to the first term of the displacement flow given in Eq. (13).

2. Through Flow

The through flow solution in the (r, θ) plane is not altered. In particular, the flow-rate coefficient $\phi = V_{r_2}/V_2$ remains unchanged in going from the physical plane to the (r, θ) plane. The appropriate solutions are then given by Eqs. (15), Ref. 1, i.e.,

$$V_{t_2} = - \frac{Q\cos\gamma}{\pi \rho_2} (\tan\gamma - \tan\alpha_1)$$

$$V_{t_1} = \frac{Q\cos\gamma}{\pi \rho_i} (\tan\gamma - \tan\alpha_1) \qquad (16)$$

where Q is the flow-rate per passage per unit width.

3. Shockless Entry

All the essential information is now available to make calculations of head flow-rate performance in which the effect of meridian curvature is taken into account. The first and most important item is the flow-rate for which shockless or smooth entry occurs on the Francis-type impellers.

This operating point is determined by the condition that the velocity must be zero in the circle plane at the point corresponding to the inlet of the blade.

According to Ref. 1 this occurs when

$$(V_{t_1} - V_{t_2}) + (V_{d_1} - V_{d_2}) + (V'_{d_1} - V'_{d_2}) = 0 . \tag{17}$$

After suitable manipulation of the equations quoted above, the flow-rate coefficient ϕ'_e for this condition may be expressed as

$$\phi'_e = \phi'_{e\infty} \left[A + \left(\frac{R_i}{R_1} \right)^2 (1 - A) \right] \tag{18}$$

where ϕ' is defined by

$$\phi' = \frac{V_{r_2}}{U_2} = \frac{\text{Flow-Rate}}{\text{Exit Area x Tip Speed}} \tag{19}$$

The subscript (∞) denotes the value of this coefficient for an infinite number of vanes, i.e.,

$$\phi'_{e\infty} = - \left[\frac{R_1}{R_2} \right]^2 \Big/ (\tan\gamma - \tan\alpha_1) .$$

The term A is the ratio $\phi'_e/\phi'_{e\infty}$ for a purely radial impeller, and is given in Ref. 1 as

$$A = \left. \frac{\phi'_e}{\phi'_{e\infty}} \right|_{\delta = 0} = \frac{1}{\psi_o} \left(1 + \frac{4\pi^2 \cos^2\gamma}{3N^2} \right) \tag{20}$$

subject to the restriction that the solidity be greater than about 1.2. The solidity for a Francis impeller is defined as

$$\sigma = \frac{N \ln r_2/r_1}{2\pi \cos\gamma} \tag{21}$$

Equation (18) appears to be independent of R_1/R_2. Actually, A depends on

σ (and thus R_1/R_2) but if the solidity is subjected to the above restriction A becomes independent of σ and is a function of the vane angle and number of blades alone. In fact, Eq. (20) is only an approximation for the case $\sigma = 1.2$, and for smaller values a more complicated relation must be used (Ref. 1).

If a large value of R_2/R_i is chosen as the tip radius in Fig. 3, the angular inclination of the exit will be essentially radial. Suppose for the moment that the radius ratio R_1/R_2 of the impeller is sufficiently small so that $\sigma \geq 1.2$. If now, R_1/R_2 is decreased below this value, the inlet edge of the blade will become more axial. Since the impeller geometry already is presumed to be such that A does not change, the sole effect on the shockless flow-rate condition is that due to a change in the inlet meridian angle δ_1. Values of (R_i/R_1) then may be substituted into Eq. (18) and the corresponding value of δ_1 determined from Fig. 4. (Actually, for these purposes, one may just as well take R_2/R_i as infinity.)

This result is independent of the exit meridian angle δ_2 if the solidity remains high. This fact may be seen in the following way: Let σ have a constant value so that $r_1 = r_1/r_2$ is also constant. Since

$$\left[\frac{R_o}{R_1}\right]^2 = \frac{1 - r_1^2 (R_2/R_i)^2}{1 - r_1^2}$$

the value of A will stay constant if r_1 is kept constant and independent of the radius ratio R_1/R_2 of the impeller. Thus, for a given r_1 (and therefore constant A) R_i/R_1 and R_2/R_1 can both approach unity and δ_2 approach 90° without affecting the value of $\phi_e/\phi_{e\infty}$ as computed by Eq. (18).

Equation (18) is plotted in Fig. 5 for the case of $N = 6$, $\gamma = 70^\circ$ which is typical of many pump designs. It is evident that the inlet meridian inclination δ_1 has a large effect and must be taken in account in any actual design.

4. Head Flow-Rate Performance

The head developed by the impeller is usually expressed by the coefficient

$$\psi = H/U_2^2/g$$

where H is the developed head, and U_2 is the tip speed of the impeller. This coefficient may be shown to be equal to

$$\psi = -N(V_{d_2} + V_{t_2})$$

ω and r_2 being unity. With the aid of Eqs. (14), (15), and (16), the head flow-rate relation becomes

$$\psi = \psi_o^* - C_H \phi(\tan\gamma - \tan\alpha_1) \tag{22}$$

for backward curved impellers where

$$\psi_o^* = \psi_o\left[1 - \left(\frac{R_i}{R_2}\right)^2\right] + C_H\left[\frac{R_i}{R_2}\right]^2 \tag{23}$$

is now the shut-off head coefficient. The coefficient C_H depends on the impeller solidity and the blade angle and is usually very near unity. The term ψ_o is the shut-off head coefficient for a straight radial configuration. Graphs of both of these coefficients are given in Ref. 1.

Equation (23) is plotted in Fig. 7 for $N = 6$ and $\gamma = 70^\circ$ with the assumption that $\sigma = 1.2$.

B. Conical Impellers

The meridian picture now appears as a simple cone. Equations (1) and (4) give

$$f'(R) = \tan\delta$$

$$r = \left[\frac{R}{R_2}\right]^{\frac{1}{\cos\gamma}} .$$

The boundary condition for the displacement flow is

$$V_{nr} = \omega\cos\gamma\, r^{2\cos\delta - 1} . \tag{24}$$

The solution of this problem is given by a value of

$$m = 2 \cos \delta - 2$$

in Eq. (35), Ref. 1. It is seen that the equivalent number of vanes to be used in Eq (38), Ref. 1, is

$$N' = \frac{2N}{m+2} = \frac{N}{\cos \delta} \tag{25}$$

Thus, the characteristics of the conical impeller are obtained by replacing the actual number of blades by the equivalent number given by Eq. (25). The shockless entry calculation gives then

$$\frac{\phi_e}{\phi_{e\infty}} = \frac{1}{\psi_o(N')} \left[1 + \frac{4\pi^2 \cos^2 \gamma}{3N'^2} \right] \tag{26}$$

These results were previously obtained in Ref. 1 by a different method and also by Prof. Wislicenus in an unpublished note.

Equation (26) is plotted on Fig. 5 for the case of $N = 6$, $\gamma = 70^\circ$. It is seen that this curve is quite close to that of Eq. (18). This agreement shows that as far as shockless entry is concerned the exact details of the meridian streamline shape are relatively unimportant and that the influence of the exit angle δ_2 is small.

The shut-off head coefficient for a conical impeller is determined by the use of the equivalent number of blades as given by Eq. 24 and Fig. 6 of Ref. 1. The effect of the cone angle on this coefficient is shown in Fig. 6 for the case $N = 6$, $\gamma = 70^\circ$ and $\sigma = 1.2$. The two curves are seen to agree quite closely as is reasonable for impellers of high solidity.

Conclusions

This analysis has shown that the flow-rate for shockless entry is strongly dependent upon the inlet meridional inclination of the blade and is

relatively independent of the shape of the meridional stream surface. The shut-off head coefficient shows a similar behavior with the exit slope.

These calculations were made for a particular profile that had a continuous axial to radial curvature, and for conical profiles. The agreement between the two was sufficiently close so that the effect of inlet and exit meridional slopes may just as well be approximated by the simpler conical shape. This result should hold true at least for shroud curvatures no sharper than the particular one studied.

References

1. Acosta, A. J., "Potential Flow through Radial Flow Turbomachine Rotors", California Institute of Technology, Hydrodynamics Laboratory Report No. E-19.4.

2. Smythe, W. R., "Static and Dynamic Electricity", 1st ed. McGraw-Hill, 1939, p. 241.

Notations

A - The flow-rate ratio $\phi_e/\phi_{e\infty}$ for a radial impeller

C_H - Flow-rate correction factor

F - Velocity potential

g - Gravitational constant

H - Impeller head (ft.)

N - Number of blades

Q - Flow rate (ft^3/sec)

R - Radial coordinate in physical plane

r - Radius in the transformed radial plane

s - Arc distance along a meridian

U - Circumferential velocity ($R\omega$)

V - Absolute velocity

y - Intermediate radial variable

z - Axial coordinate in physical plane

α - Angle between absolute velocity and meridian (positive increasing counter-clockwise)

γ - Angle between blade tangent and meridian

δ - Angle between radial line and tangent to meridian

θ - Polar angle about axis of rotation

σ - Solidity - $\dfrac{N \ln r_2/r_1}{2\pi \cos\gamma}$

ϕ - Flow-rate coefficient, $\dfrac{\text{Discharge}}{\text{Exit area x tip speed}} = \dfrac{V_{m2}}{U_2}$

ψ - Head coefficient, $H/U_2^2/g$

ψ_o^* - Shut-off head coefficient

ψ_o - Shut-off head coefficient for a purely radial impeller

ω - Angular speed

Subscripts

d - Refers to displacement flow

e - Denotes shockless or smooth entry

n - Normal component of velocity

m - Meridional component of velocity

r - Refers to (r, θ) plane

s - Refers to (s, θ) plane

t - Refers to through flow

1 - Refers to vane inlet

2 - Refers to vane exit or tip

∞ - Denotes the infinite vane theory

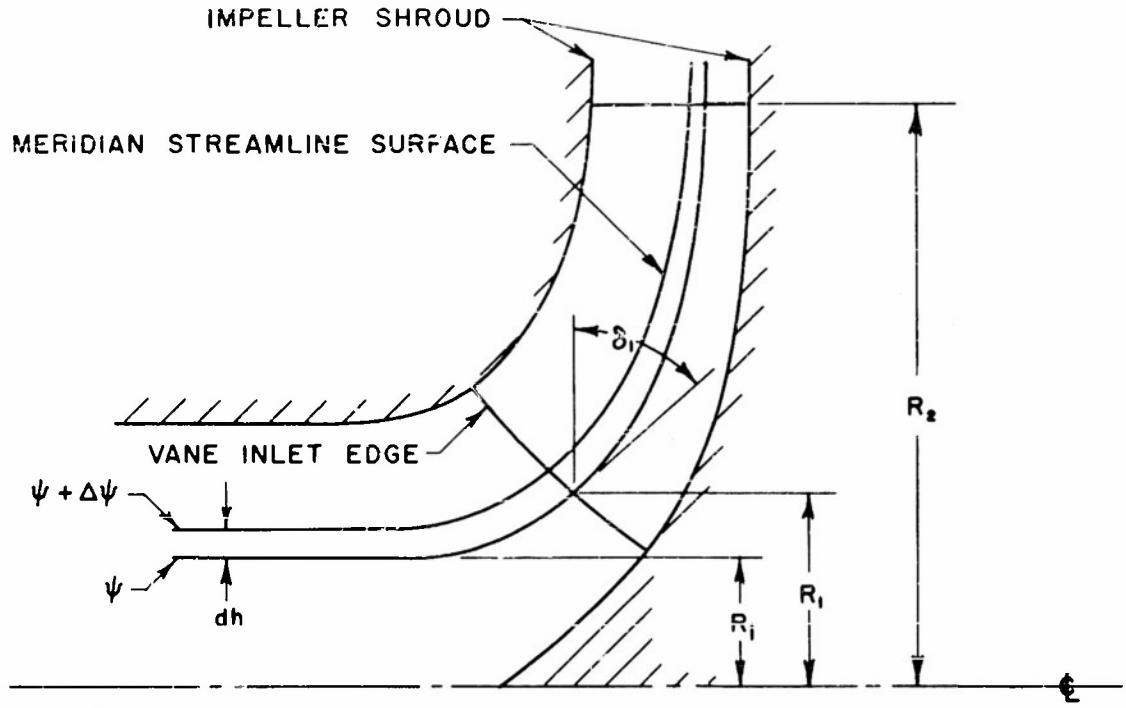

Fig. 1 - Meridian profile of a Francis type impeller.

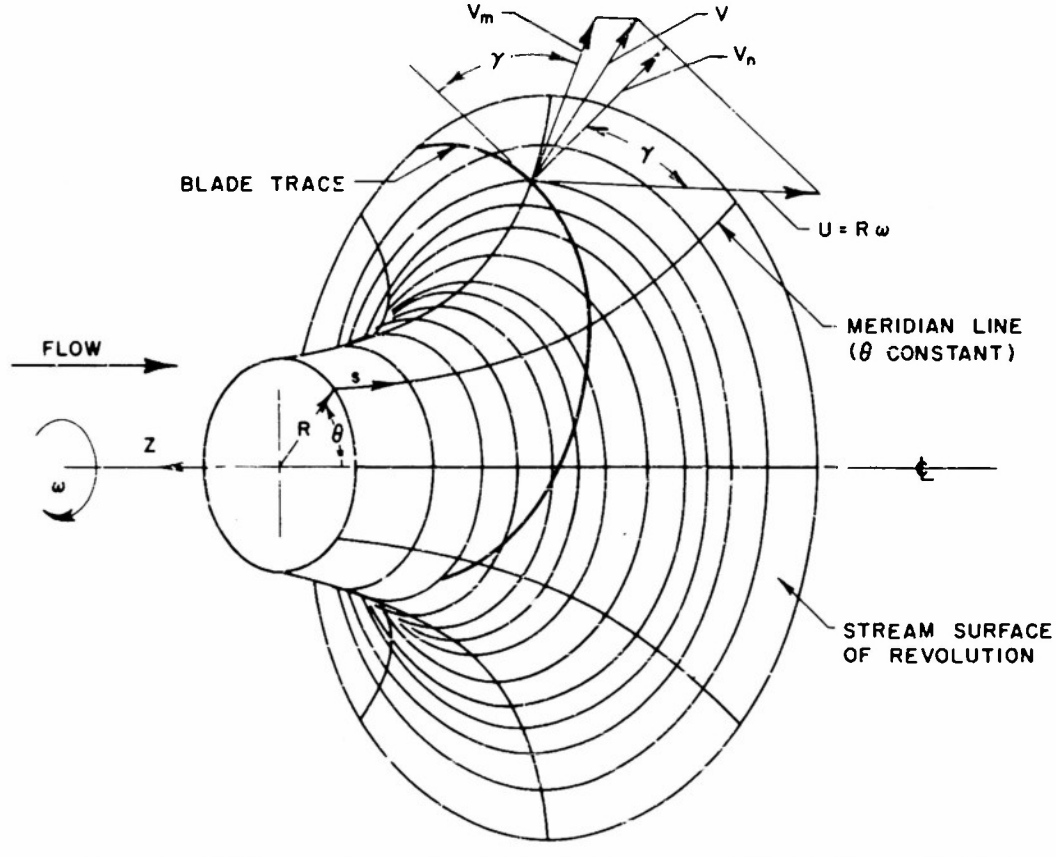

Fig. 2 - Oblique view of a typical stream surface of revolution showing the blade trace and coordinate system.

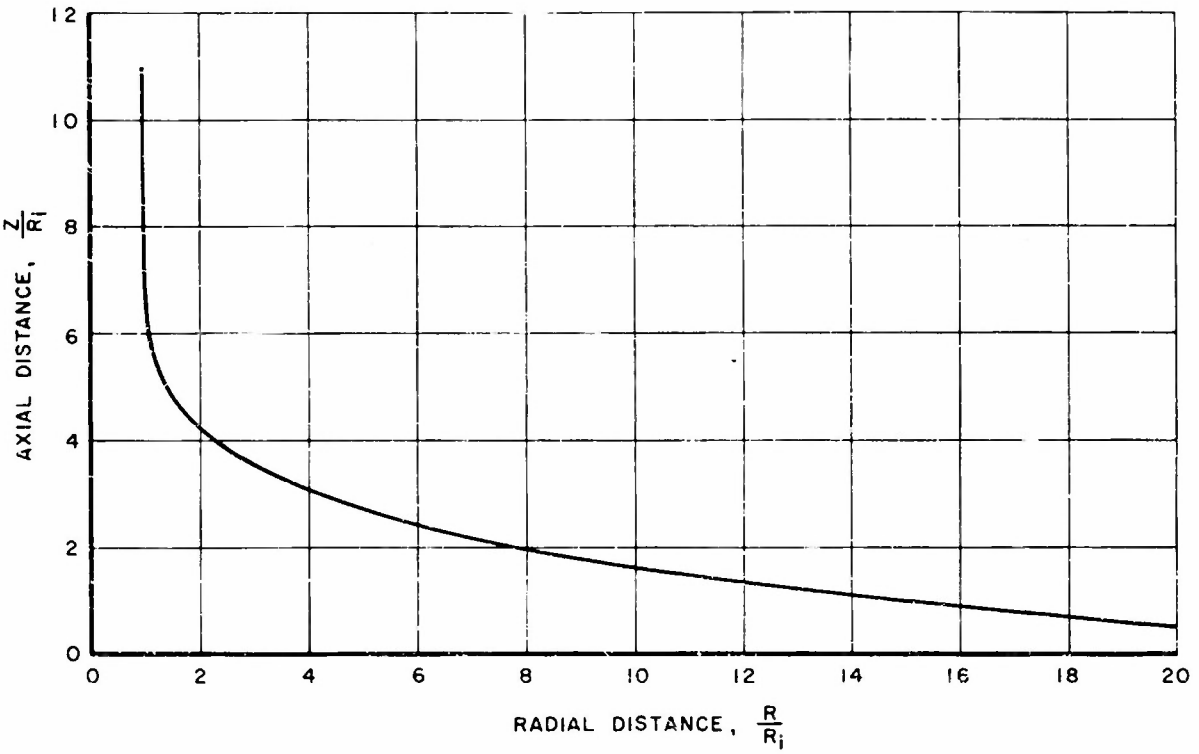

Fig. 3 - Plot of axial distance vs. radius for the special stream surface given by Eq. 10.

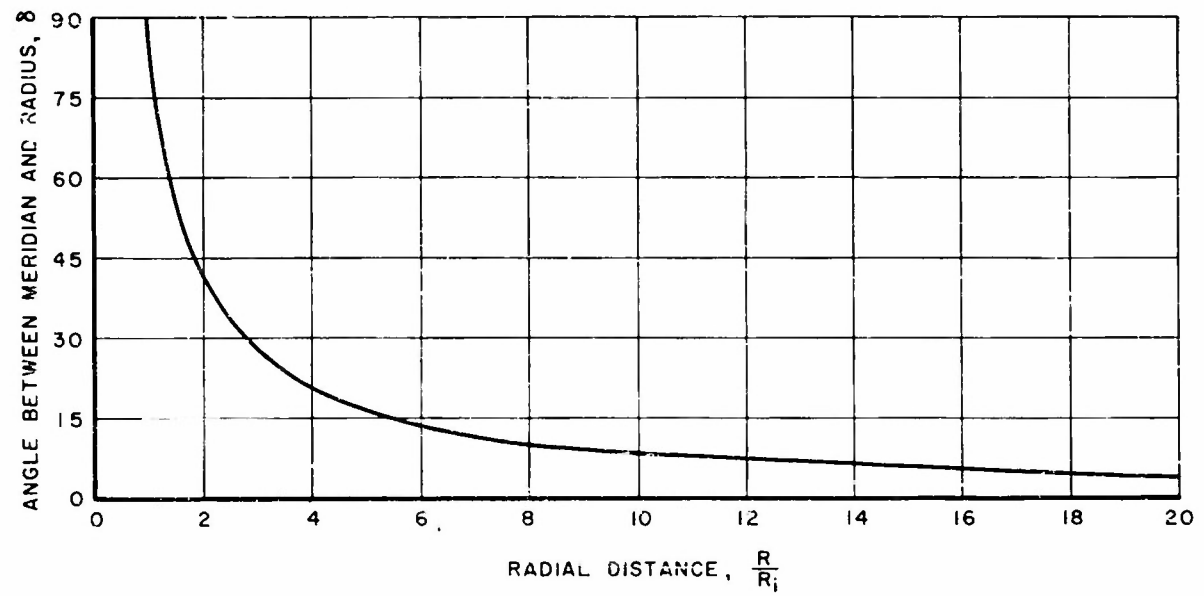

Fig. 4 - Meridian inclination δ for the shape shown in Fig. 3.

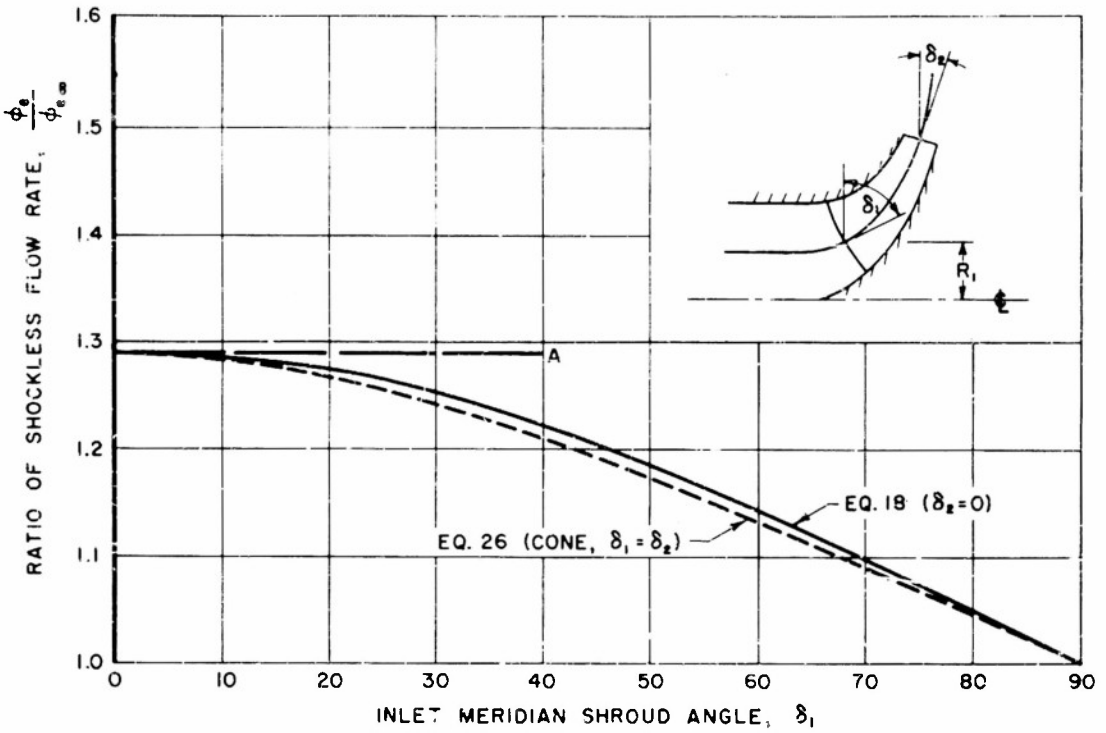

Fig. 5 - Ratio of shockless flow rates vs. inlet meridian shroud angle δ_1 for the case of 6 blades, $\gamma = 70^\circ$ and solidity = 1.2.

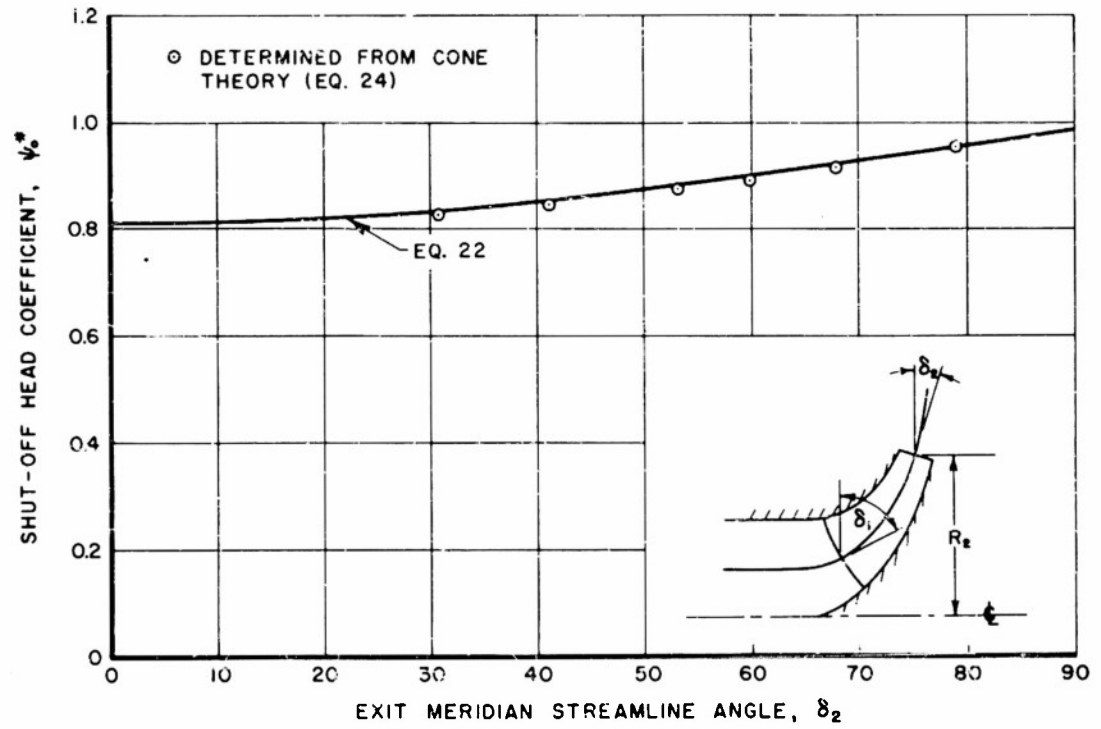

Fig. 6 - Shut-off head coefficient ψ_o^* vs. exit meridian shroud angle δ_2 for the case of 6 blades, $\gamma = 70^\circ$ and solidity = 1.2.

DISTRIBUTION LIST - CONTRACT N6onr-24402
Hydrodynamics Laboratory
California Institute of Technology

Chief of Naval Research
Department of the Navy
Washington 25, D.C.
Attn: Code 429 1
Code 438 2

Commanding Officer
Office of Naval Research
Branch Office
John Crerar Library Bldg.
86 E. Randolph Street
Chicago 1, Illinois 1

Commanding Officer
Office of Naval Research
Branch Office
346 Broadway
New York 13, New York 1

Commanding Officer
Office of Naval Research
Branch Office
1030 E. Green Street
Pasadena 1, California 2

Commanding Officer
Office of Naval Research
Branch Office
1000 Geary Street
San Francisco, California 1

Chief, Bureau of Aeronautics
Department of the Navy
Washington 25, D.C.
Attn: Research Division 1

Chief, Bureau of Ordnance
Dept. of the Navy
Washington 25, D.C.
Attn: Code Re6a 1
Research and Development
Division 1

Commanding Officer
Naval Ordnance Laboratory
White Oak, Silver Spring, Md. 1

Commander
Naval Ordnance Test Station
3202 E. Foothill Blvd.
Pasadena, California
Attn: Mr. J. Neustein 1

Commanding Officer
Naval Torpedo Station
Keyport, Washington 1

Chief, Bureau of Ships
Department of the Navy
Washington 25, D.C.
Attn: Research Div. 1
Prop and Shaft Branch 1

Documents Service Center
Armed Services Technical
Information Agency
Knott Building
Dayton 2, Ohio 5

Director
Naval Research Laboratory
Washington 20, D.C.
Attn: Code 2021 1

Commanding Officer and Director
David Taylor Model Basin
Washington 7, D.C.
Attn: Hydromechanics Lab. 1
Hydromechanics Div. 1
Ship Div. 1
Technical Library 1

Commanding General
Office of Ordnance Research
Department of the Army
Washington 25, D.C. 1

Directorate of Intelligence
Headquarters, U.S. Air Force
Washington 25, D.C.
Attn: Director, Research and
Development 1

Commanding General
Air Research and Development
Command
Office of Scientific Research
Post Office Box 1395
Baltimore 3, Maryland 1

Distribution List - Contract N6onr-24402 (continued)
Hydrodynamics Laboratory
California Institute of Technology

Director of Research
National Advisory Committee for Aeronautics
1724 F Street, Northwest
Washington, D.C.
Attn: Director of Research 1

Director
Langley Aeronautical Laboratory
National Advisory Committee for Aeronautics
Langley Field, Virginia 1

Director
Ames Aeronautical Laboratory
National Advisory Committee for Aeronautics
Moffett Field, California 1

Director
Lewis Flight Propulsion Laboratory
National Advisory Committee for Aeronautics
21000 Brookpark Road
Cleveland 11, Ohio 1

Director
National Bureau of Standards
National Hydraulic Laboratory
Washington 25, D.C.
Attn: Dr. G. B. Schubauer 1

Polytechnic Institute of Brooklyn
Dept. of Aeronautical Engineering and Applied Mechanics
99 Livingston Street
Brooklyn 2, New York
Attn: Professor A. Ferri 1
: Professor H. J. Reissner 1

Polytechnic Institute of Brooklyn
Dept. of Mechanical Engineering
99 Livingston Street
Brooklyn 2, New York
Attn: Professor C.H. Wu 1

The Johns Hopkins University
Dept. of Mechanical Engineering
Baltimore 18, Maryland
Attn: Dr. G. F. Wislicenus 1

Massachusetts Institute of Technology
Hydrodynamics Laboratory
Cambridge 39, Mass.
Attn: A. T. Ippen 1

Massachusetts Institute of Technology
Dept. of Naval Architecture
Cambridge 39, Mass. 1

Massachusetts Institute of Technology
Department of Mechanical Engineering
Cambridge 39, Mass.
Attn: Professor E. S. Taylor 1

Ordnance Research Laboratory
Pennsylvania State College
State College, Pennsylvania
Attn: Dr. J. M. Robertson 1

Princeton University
Department of Mechanical Engineering
Princeton, New Jersey
Attn: Professor C. P. Kittridge 1

State University of Iowa
Iowa Institute of Hydraulic Research
Iowa City, Iowa
Attn: Dr. Hunter Rouse, Director 1

Experimental Towing Tank
Stevens Institute of Technology
711 Hudson Street
Hoboken, New Jersey 1

University of California
Department of Mechanical Engineering
Los Angeles, California
Attn: Dr. H. A. Einstein 1

University of Maryland
Institute for Fluid Mechanics and Applied Mathematics
College Park, Maryland
Attn: Professor J. R. Weske 1

University of Minnesota
St. Anthony Falls Hydraulic Laboratory
Minneapolis 14, Minnesota
Attn: Dr. L. G. Straub 1

University of Notre Dame
College of Engineering
Notre Dame, Indiana
Attn: Dr. K. E. Schoenherr, Dean 1

Distribution List - Contract N6onr-24402 (continued)
Hydrodynamics Laboratory
California Institute of Technology

University of Tennessee
Engineering Experimental Station
Knoxville, Tennessee
Attn: Dr. G. H. Hickox
Associate Director 1

Worcester Polytechnic Institute
Alden Hydraulic Laboratory
Worcester, Mass.
Attn: Professor L. J. Hooper 1

Aerojet General Corporation
6352 Irwindale Avenue
Azusa, California
Attn: Mr. C. A. Gongwer 1

California Institute of Technology
Jet Propulsion Laboratory
Pasadena 4, California 1

Commanding Officer
Office of Naval Research
Navy 100, Fleet Post Office
New York, New York 1

Editor, Biblography of Technical Reports
Office of Technical Services
U.S. Dept. of Commerce
Washington 25, D.C. 1

Editor, Technical Data Digest
Armed Services Technical Information Agency
Document Service Center
U.B. Building
Dayton 2, Ohio 1

Editor, Engineering Index
29 West 39th Street
New York 18, N.Y.

Editor, Aeronautical Engineering Review
2 E. 64th Street
New York 21, N.Y. 1

Editor, Applied Mechanics Reviews
Midwest Research Institute
4049 Pennsylvania Avenue
Kansas City 2, Missouri 2

Technical Library
Lockheed Aircraft Corp.
2555 North Hollywood Way
Burbank, California 1

Technical Library
Pratt and Whitney Aircraft Div.
United Aircraft Corp.
East Hartford 8, Conn. 1

Technical Library
Glenn L. Martin Company
Baltimore 3, Maryland 1

Technical Library
Grumann Aircraft Engineering Corp.
Bethpage, Long Island, N. Y. 1

Technical Library
McDonnell Aircraft Corp.
Box 516
St. Louis 3, Missouri 1

Technical Library
North American Aviation, Inc.
12241 Lakewood Blvd.
Downey, California 1

Technical Library
Northrop Aircraft Company
1017 E. Broadway
Hawthorne, California 1

Prof. H. Emmons
Harvard University
Cambridge 38, Mass. 1